Behavior of Torsionally Coupled Structures with Variable Frequency Pendulum Isolator

Pranesh Murnal[1] and Ravi Sinha, M.ASCE[2]

Abstract: The essential characteristics of an effective base isolation system are isolation, energy dissipation, and restoring mechanism. Some friction type base isolation systems proposed earlier have been found to be very effective in reducing the structural response and incorporate simple restoring mechanisms through gravity. However these isolators are effective only under certain excitation and structural characteristics. To overcome these limitations the authors have recently developed a new isolation system called the variable frequency pendulum isolator (VFPI) that has been found to be very effective under a variety of structure and excitation characteristics. In this paper, the mathematical formulation for the three dimensional behavior of an asymmetric structure isolated by a sliding type isolator, with particular reference to VFPI has been presented. The behavior of torsionally coupled structure isolated by VFPI has been examined. The factors affecting the torsional coupling of isolated structure have been identified. The behavior of structure isolated by VFPI has been compared with the structure isolated by other type of friction isolators such as friction pendulum system and pure-friction system.

DOI: 10.1061/(ASCE)0733-9445(2004)130:7(1041)

CE Database subject headings: Structural control; Base isolation; Torsional vibration; Energy dissipation; Passive control; Vibration control.

Introduction

Aseismic design of structures using base isolation systems is an area of extensive research and development. Base isolation systems use a flexible layer at the base of the structure, which allows relative displacements between the foundation and the superstructure. Due to the addition of an isolation layer, the fundamental time period of the structure lengthens so as to move away from the dominant time periods of ground motions, thereby reducing the acceleration induced in the structure. A detailed review of base isolation concepts and applications is available in published literature (Kelly 1986; 1993b; Buckle and Mayes 1990; Naeim and Kelly 1999).

Practical applications of base isolation devices incorporate energy dissipation in addition to isolation so as to limit deformations at the isolation level during ground excitations. For instance, in friction-type base isolators, isolation is achieved through sliding while energy is dissipated through sliding friction. These isolation devices are found to substantially reduce the structural accelerations, and the performance of these isolators is also relatively insensitive to severe variations in the frequency and amplitude of ground motions (Mostaghel and Tanbakuchi 1983). However, the use of simple sliding isolator (pure-friction system) may result in large sliding and residual displacements (permanent displacement at the end of ground motion) of the structure, which are difficult to incorporate in practical design. This limitation of isolation system can be overcome by introducing a suitable restoring mechanism in the isolation system to bring the structure back to its original position after the end of ground excitations. One of the most robust restoring mechanisms has been used in friction pendulum system (FPS). The FPS uses a spherical sliding surface that incorporates restoring mechanism through gravity (Zayas et al. 1987, 1990). Though versatile and widely used, this system has some inherent limitations and is useful for a limited range of structure and isolator characteristics (Pranesh 2000).

A new isolation device called the variable frequency pendulum isolator (VFPI) that incorporates the advantages of FPS and pure-friction (PF) system has been recently developed (Sinha and Pranesh 1998; Pranesh and Sinha 2000a). The essential characteristics of VFPI include its ability to change the fundamental time period of isolated structure with sliding displacement, and its ability to limit the maximum lateral force transmitted to the structure due to ground motions. The performance of VFPI based on numerical simulations is found to be very effective for a wide range of different structure and excitation characteristics with clear advantages over other sliding isolation systems (Pranesh and Sinha 2000b, 2002; Sinha and Pranesh 2001).

The practical effectiveness of performance of base-isolated structures is strongly influenced by its torsional behavior. Almost all structures experience three-dimensional response during ground motions due to lack of symmetry between the structure's center of rigidity (CR) and center of mass (CM). In several situations, one or more dominant lateral natural frequencies of the structure may tune with its torsional frequency. Tuning is also often observed in isolated structures, due to isotropic behavior of the isolators, if there is an imbalance between the CM and the CR (Kelly 1993a). Several researchers have investigated the coupled lateral–torsional response of fixed base and base-isolated buildings (Lee 1980; Pan and Kelly 1983; Goel and Chopra 1990; Nagarajaiah et al. 1993; Jangid and Datta 1994). Most investiga-

[1]Professor, Government College of Engineering, Karad, Maharashtra, India. E-mail: pmurnal@yahoo.com

[2]Professor, Indian Institute of Technology Bombay, Powai, Mumbai-400076, India (corresponding author). E-mail: rsinha@iitb.ac.in

Note. Associate Editor: Andrei M. Reinhorn. Discussion open until December 1, 2004. Separate discussions must be submitted for individual papers. To extend the closing date by one month, a written request must be filed with the ASCE Managing Editor. The manuscript for this paper was submitted for review and possible publication on April 26, 2002; approved on August 18, 2003. This paper is part of the ***Journal of Structural Engineering***, Vol. 130, No. 7, July 1, 2004. ©ASCE, ISSN 0733-9445/2004/7-1041–1054/$18.00.

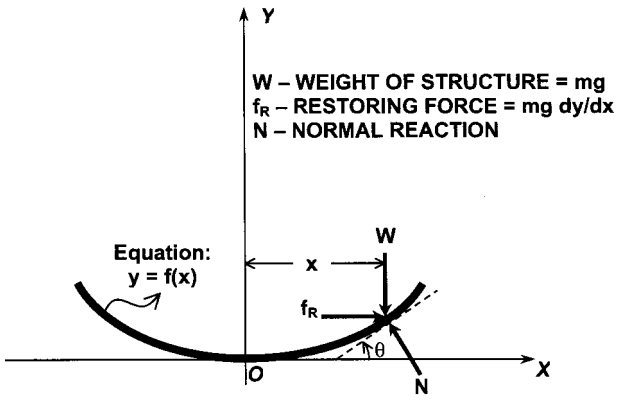

Fig. 1. Free body diagram of smooth sliding surface of isolator

tions have found that torsional coupling significantly affects the behavior of base isolated structure and this effect needs to be rigorously considered in analysis and design.

In this paper the mathematical formulation for the response of a three-dimensional (3D) structure with sliding isolators has been presented. The standard formulation for three-dimensional response has been modified to account for nonlinear restoring force developed by VFPI. The formulation has been presented in state space, which requires complex modal analysis, whose close-form solution of uncoupled equations of motion can directly provide the response. The concept of rotational sliding and its condition for occurrence has also been presented in this paper. The behavior of torsionally coupled three-dimensional structures with rigid diaphragms has been investigated and the important parameters affecting torsional response have been identified. The performance of VFPI has been compared with that of FPS and PF systems for example structures, and the response has been also compared with that of a fixed-base structure.

Variable Frequency Pendulum Isolator Geometry

Consider a rigid mass m moving on a smooth curved surface with co-ordinate axes as defined in Fig. 1. The restoring force at any position of the mass is given by

$$f_R = mg\frac{dy}{dx} \tag{1}$$

If the restoring force is assumed to be offered by a nonlinear spring of instantaneous stiffness $k(x)$ then the restoring force is expressed as

$$f_R = k(x)x \tag{2}$$

Defining an instantaneous frequency for the sliding surface as $\omega_b(x)$, the above equation can be written as

$$f_R = m\omega_b^2(x)x \tag{3}$$

where the instantaneous frequency depends solely on the geometry of the sliding surface.

The geometry of sliding surface of VFPI has been devised from the characteristics of an elliptical geometry. The equation of an ellipse symmetrical about vertical axis and with its origin as defined in Fig. 1 is given by

$$y = b(1-\sqrt{1-x^2/a^2}) \tag{4}$$

where a and b = semimajor and semiminor axes of the ellipse, respectively. Differentiating Eq. (4) we get

$$\frac{dy}{dx} = \frac{b}{a^2\sqrt{1-x^2/a^2}}x \tag{5}$$

Now, referring to Eqs. (1), (3), and (5) the frequency of the isolator can be expressed as

$$\omega_b^2(x) = \frac{\omega_I^2}{\sqrt{1-x^2/a^2}} \tag{6}$$

where $\omega_I^2 = gb/a^2$ = square of the initial frequency at zero horizontal displacement. From the above expression it is seen that the frequency of an elliptical sliding curve depends on the ratio b/a^2 [Eq. (6)]. That implies that for a fixed value of minor axis b, the frequency decreases with the increase in the value of the semimajor axis a. So, a new geometry for the sliding surface of the isolator can be formulated by taking the semimajor axis a, a linear function of x, so that the frequency of the isolator sharply decreases with the increase in sliding displacement. This is equivalent to an infinite number of ellipses continuously transforming in to one another such that the semimajor axis is larger for larger sliding displacement and ratio b/a^2 approaches a value zero at infinity. Mathematically, semimajor axis a can be represented as

$$a = x + d \tag{7}$$

where x = sliding displacement and d = positive constant. Substituting Eq. (7) in Eq. (4) and simplifying, we get

$$y = b\left[1-\frac{\sqrt{d^2+2dx\ \mathrm{sgn}(x)}}{d+x\ \mathrm{sgn}(x)}\right] \tag{8}$$

In the above equation signum function has been introduced to maintain symmetry of the curve about the vertical axis. This is equivalent to rotating the curve about the vertical axis, to get the required three-dimensional sliding surface. The signum function has a value of $+1$ for positive value of x and -1 for negative value of x. The introduction of signum function in Eq. (8) ensures that the term under the square root remains positive for all values of x. It is observed that this equation gives a curve, which has a maximum vertical ordinate equal to b that occurs only at infinity. The parameter d determines the initial value of the semimajor axis (which is greater than zero) and the semimajor axis increases with displacement x, as seen from Eq. (7). Now by differentiating, the slope of the curve at any point is given by

$$\frac{dy}{dx} = \frac{bd}{[d+x\ \mathrm{sgn}(x)]^2\sqrt{d^2+2dx\ \mathrm{sgn}(x)}}x \tag{9}$$

For notational convenience, we define $r = x\ \mathrm{sgn}(x)/d$. The sliding frequency can be expressed as

$$\omega_b^2(x) = \frac{\omega_I^2}{(1+r)^2\sqrt{1+2r}} \tag{10}$$

In the above equations, b and d = geometric parameters that completely define the isolator properties. The ratio b/d^2 determines the initial frequency of the isolator and the value of d decides the rate of variation of the isolator frequency. Since the rate of variation of isolator frequency depends only on $1/d$, the factor $1/d$ has been defined as frequency variation factor (FVF). A higher value of FVF will result in steeper variation of the isolator frequency. When the FVF is very large (d tending to zero) the rate of decrease in frequency with sliding displacement is so rapid that

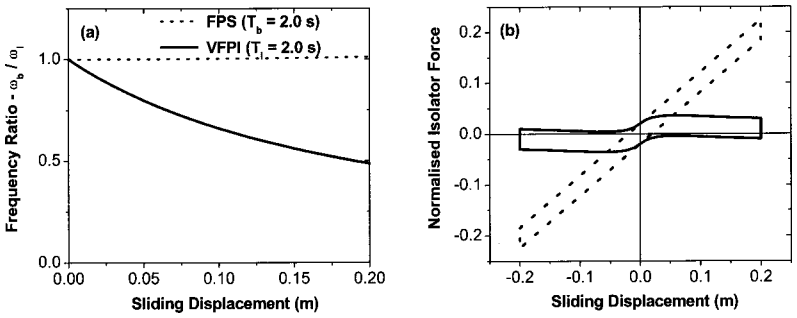

Fig. 2. Frequency and restoring force characteristics of variable frequency pendulum isolator and friction pendulum system: (a) frequency ration and (b) normalized isolator force

the frequency tends to zero immediately and the surface is almost flat (similar to a PF system). On the other hand if FVF is very small (very large value of d), the frequency variation with sliding displacement is negligible and it represents a nearly constant frequency surface similar to FPS. Therefore an optimum value of FVF can incorporate the advantages of both these systems.

The variation of isolator frequency and the hysteretic curve are shown in Figs. 2(a and b), for typical values of parameters b (0.09 m) and d (0.30 m) and an initial isolator period of 2 s. From this figure it can be observed that the frequency decreases sharply with the sliding displacement and also the force–deformation relation shows a softening of the restoring force for higher sliding displacements. The isolator with its sliding surface defined by Eq. (8) has been called the VFPI (Pranesh and Sinha 2000a). It should be noted that all positive constant values of d are admissible in the formulation.

The VFPI has two distinguishing characteristics that makes it more effective than the other friction type isolators: (1) the frequency of the isolator decreases with increase in sliding displacement so as to provide larger separation between the structure and the excitation frequencies (resulting in continuous mismatch of frequencies), and (2) the isolator restoring force exhibits softening for large sliding displacements and the maximum transmitted force is bounded. The second characteristic results in transmission of smaller forces to the structure during high level of excitation and provides a fail-safe mechanism (Pranesh and Sinha 2000a, 2002).

Due to the varying geometry of sliding surface, the contact between the slider and sliding surface of VFPI may be not uniform. In practical implementation, this may result in excessive wear and tear and/or local damage to the sliding surface. These issues and their implications have not been included in the formulation, and have not been discussed in the paper.

Mathematical Modeling of Three Dimensional Isolated Structure

Consider a base isolated rigid floor building with N floors. The motion of each floor can be defined using three master degrees-of-freedom (DOFs) at the center of mass of the floors; two lateral translational DOFs in the horizontal direction and one rotational DOF (Fig. 3). At the isolator level all the isolators are assumed to be rigidly connected. As a result, the motion of an isolator can be expressed in terms of the three master degrees-of-freedoms at the center of base mass. The lateral and torsional stiffness can be calculated from the properties of lateral load-resisting elements using conventional procedures (Chopra 2000). The torsional stiffness at the isolator level is the stiffness due to isolator restoring force alone (due to the curved sliding surface), neglecting the frictional force. In the formulation of equations of motion of multidegrees-of-freedom structures, the equivalent stiffness due to isolator restoring force is included in the stiffness matrix while the frictional force is considered as a driving force (Pranesh and Sinha 2002).

A structure may be supported on a large number of isolators, and the motion of each isolator has to be evaluated separately. Consider the jth isolator, the position of which is defined by X_j

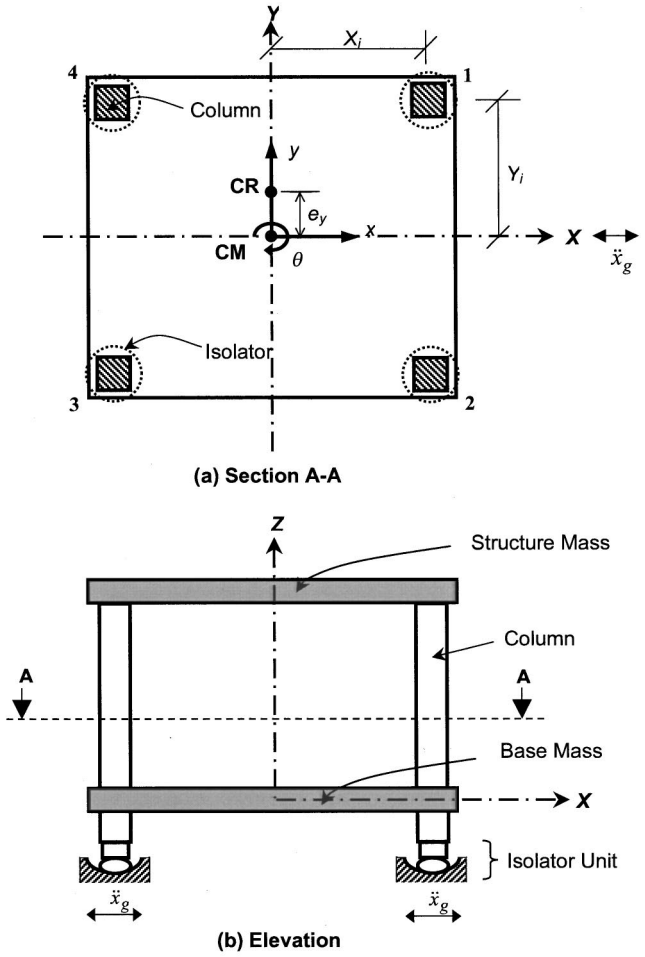

Fig. 3. Schematic plan and elevation of asymmetric structure considered in this study

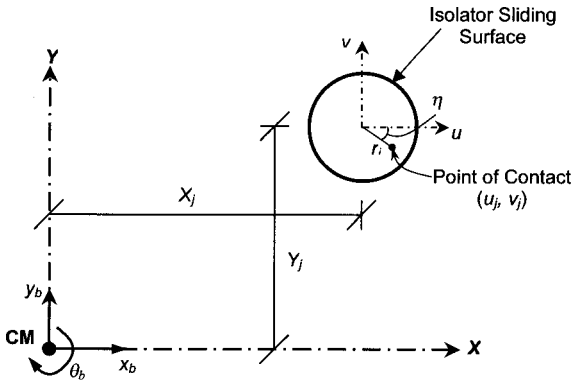

Fig. 4. Coordinate system for jth individual isolator (showing plan view of isolator 1 located in upper right quadrant of Fig. 3)

and Y_j as shown in Fig. 4. The displacements of CM of the base are defined by vector $\mathbf{x_b}$, consisting of the two translation components x_b and y_b, and one rotation component θ_b. The displacements at an isolator can be defined by a local coordinate system with coordinates u_j and v_j relative to the center of the sliding surface as shown in Fig. 4. As all the isolators are rigidly connected to the base, the displacement of any isolator can be expressed in terms of the displacements of the CM of the base mass as

$$u_j = x_b - \theta_b Y_j$$
$$v_j = y_b + \theta_b X_j \tag{11}$$

The restoring force in any isolator depends on the values of isolator sliding displacements u_j and v_j. The restoring force acting along the radial direction (towards the center of the sliding surface) at the jth isolator for any position of the slider is given by

$$f_R^j = W_j \frac{dy_{hj}}{dr_j} \tag{12}$$

where W_j = vertical force on the jth isolator (Fig. 1); y_{hj} = vertical displacement along the sliding surface; and $r_j = \sqrt{u_j^2 + v_j^2}$ = radial displacement of the slider from center of the sliding surface. Representing this restoring force in the jth isolator by an equivalent nonlinear spring force, it can be expressed as

$$f_R^j = k(r_j) r_j \tag{13}$$

in which $k(r_j)$ = equivalent nonlinear spring stiffness. The spring stiffness can be further written as

$$k(r_j) = m_j \omega_b^2(r_j) \tag{14}$$

where m_j = mass equivalent to vertical force ($m_j = W_j/g$); and $\omega_b(r_j)$ = instantaneous frequency of the isolator, which depends on radial displacement r_j. The isolator restoring force can be resolved along two principal directions as

$$f_{Rx}^j = k(r_j) r_j \cos\eta$$
$$f_{Ry}^j = k(r_j) r_j \sin\eta \tag{15}$$

where η = angle made by the radial displacement with the principle x direction as shown in Fig. 4. These forces can be further expressed as

$$f_{Rx}^j = k(r_j) u_j$$
$$f_{Ry}^j = k(r_j) v_j \tag{16}$$

in which u_j and v_j = sliding displacements of the jth isolator in the two principal orthogonal directions. It has to be noted that the stiffness of the isolator for a given position is same in both the principal directions. The total restoring forces at the CM of the base due to all the isolators in the two principal directions is simply the algebraic sum of the forces in each individual isolator and can be expressed as

$$f_{Rx} = \sum_j f_{Rx}^j$$
$$f_{Ry} = \sum_j f_{Ry}^j \tag{17}$$

The point through which these forces act can be termed as the center of stiffness of the isolation system (CSI). The position of this point with respect to the CM of the base can be defined in terms of isolation eccentricities and is given by

$$e_{bx} = \frac{1}{f_{Ry}} \sum_j f_{Ry}^j X_j$$
$$e_{by} = \frac{1}{f_{Rx}} \sum_j f_{Rx}^j Y_j \tag{18}$$

It is important to note that these eccentricities are functions of the base displacements and vary with time if the isolator restoring force is nonlinear, as is the case with VFPI. For a given position of isolators with respect to CM and a given distribution of effective mass on the isolators, the eccentricity depends on the restoring force. Since the restoring force appears both in the numerator and denominator of Eq. (18), for a predominant linear motion of isolators the variation in the eccentricity can be negligible only if linear motions are involved. In the presence of torsional motions these variations may be significant. The present formulation implicitly considers this variation by evaluating the isolation forces at each time step.

Structural Response

The response of a three-dimensional structure includes components in all three orthogonal directions. Due to this reason, it is possible to formulate analysis procedure for generalized base excitations that consist of all three components of ground motions. In this section, the generalized response formulation has been presented for an N-story shear structure isolated by sliding type isolators. The motion consists of two phases, namely nonsliding phase and sliding phase and the formulation is entirely different in the two phases due to the inclusion of DOFs of the base in sliding phase only. It should be noted that when the excitation consists of a single component of ground motion, appropriate components of the excitation vector are assigned zero values and the same mathematical formulation presented herein can be used.

Nonsliding Phase

In this phase the structure behaves as a conventional fixed-base structure as there is no relative movement at the isolator level and hence the normal dynamic analysis using modal decomposition can be carried out (Chopra 2000). The equations of motion in this

phase are as given:

$$\mathbf{M_0}\ddot{\mathbf{x}}_\mathbf{0}+\mathbf{C_0}\dot{\mathbf{x}}_\mathbf{0}+\mathbf{K_0}\mathbf{x_0}=-\mathbf{M_0}\mathbf{r_0}\ddot{\mathbf{x}}_\mathbf{g} \tag{19}$$

$$\mathbf{x_b}=\text{constant}$$

and

$$\dot{\mathbf{x}}_\mathbf{b}=\ddot{\mathbf{x}}_\mathbf{b}=\mathbf{0} \tag{20}$$

where $\mathbf{M_0}$, $\mathbf{C_0}$, and $\mathbf{K_0}$ = mass, damping, and stiffness matrices (of order $3N$) of the fixed-base structure, respectively; $\mathbf{x_0}$ = vector of displacements of the structure DOFs (defined at the mass center of the floors) relative to the base (excluding the DOFs of base mass), $\mathbf{x_b}$ = displacement vector consisting of three displacement components of the base mass relative to the ground; and overdots indicate derivative with respect to time. In the above equation, $\mathbf{r_0}$ = influence coefficient matrix pertaining to the three components of ground motion and the vector $\ddot{\mathbf{x}}_\mathbf{g}$ consists of the three components of ground motions (two translations and one rotation). Eqs. (11) and (12) can be easily solved by standard modal analysis procedures to obtain the time history of the response.

Beginning of Sliding Phase

In a 3D structure isolated by sliding type of isolator two types of sliding can occur: (1) translational sliding and (2) rotational sliding. These motions are defined for the base mass supported on all isolators. It should however be noted that the motion of any given isolator is always translational. Since the motion of the base is characterized by the motion of its CM and the motion of the individual isolators in turn are dependent on the motion of the CM, the structure is assumed to be in a sliding phase whenever relative velocity corresponding to any DOF of the base mass has a nonzero value. Therefore the condition for the two types of sliding may be derived in terms of the total inertia, restoring, and frictional forces.

Translational Sliding

Translational sliding of the base mass occurs when resultant of the total inertia force and the total restoring force of the isolators equals or exceeds the total frictional force. The condition for beginning of translational sliding can be expressed as (Pranesh 2000)

$$|\sqrt{(f_{Ix}+f_{Rx})^2+(f_{Iy}+f_{Ry})^2}|\geqslant m_t\mu g \tag{21}$$

where, f_{Ix} and f_{Iy} = total inertia forces of all the masses in x and y directions, respectively; m_t = total mass of the structure; μ = coefficient of friction; and g = acceleration due to gravity. The direction of the sliding at any instant is given by

$$\tan\upsilon=\frac{f_{Iy}+f_{Ry}}{f_{Ix}+f_{Rx}} \tag{22}$$

where υ = angle of the resultant motion of the CM of base mass.

Rotational Sliding

Rotational sliding occurs when the algebraic sum of the inertial moment and the moment due to the restoring forces about the CM equals or exceeds the limiting moment required to overcome the frictional forces at the isolators. If m_i is the mass supported by ith isolator, the magnitude of limiting frictional moment is given by the sum of moments of frictional forces at the individual isolators about CM. This can be expressed as (Pranesh 2000)

$$M_f=\sum_{i=1}^{N} m_i g\mu R_i \tag{23}$$

where R_i = radial distance of the slider of the isolator from CM of the base. The condition for the rotational sliding can then be expressed as

$$|M_I+M_R|\geqslant M_f \tag{24}$$

where M_I = sum of the inertial moments of all the masses and is given by

$$M_I=\left(\sum_{i=1}^{N} I_i\ddot{\theta}_i\right)+I_b\ddot{\theta}_b \tag{25}$$

and

$$M_R=f_{Rx}\,e_{by}+f_{Ry}\,e_{bx} \tag{26}$$

In the above equations I_i = mass moment of inertia of ith mass. The beginning of a sliding phase through the rotational sliding is possible only if rotational ground motion component is dominant. Once translational sliding has been initiated the rotation of the base mass is governed by the frictional and restoring forces acting at the CSI. So, inequality (24) is applicable only at the beginning of a sliding phase.

Sliding Phase

When at least one of the inequalities (21) or (24) is satisfied the structure enters a sliding phase and the three DOFs corresponding to the base are also activated. The equations of motion are given by

$$\mathbf{M}\ddot{\mathbf{x}}+\mathbf{C}\dot{\mathbf{x}}+\mathbf{K}\mathbf{x}=-\mathbf{M}\mathbf{r}\ddot{\mathbf{x}}_\mathbf{g}-\mathbf{r}\boldsymbol{\mu}_\mathbf{f} \tag{27}$$

where $\mathbf{M}$, $\mathbf{C}$, $\mathbf{K}$ = modified mass, damping, and stiffness matrices of order $3(N+1)$; $\mathbf{r}$ = influence coefficient matrix; and $\boldsymbol{\mu}_\mathbf{f}$ = vector of frictional forces as given below

$$\mathbf{M}=\begin{bmatrix}\mathbf{M_0} & \mathbf{M_0}\mathbf{r_0}\\ [\mathbf{M_0}\mathbf{r_0}]^T & \mathbf{M_t}\end{bmatrix}$$

$$\mathbf{C}=\begin{bmatrix}\mathbf{C_0} & \mathbf{0}\\ \mathbf{0} & \mathbf{C_b}\end{bmatrix}$$

$$\mathbf{K}=\begin{bmatrix}\mathbf{K_0} & \mathbf{0}\\ \mathbf{0} & \mathbf{K_b}\end{bmatrix}$$

$$\mathbf{M_t}=\begin{bmatrix}m_t & 0 & 0\\ 0 & m_t & 0\\ 0 & 0 & I_t\end{bmatrix},\quad \mathbf{x}=\begin{Bmatrix}\mathbf{x_0}\\ \mathbf{x_b}\end{Bmatrix}$$

and

$$\mathbf{r}=\begin{bmatrix}\mathbf{0}\\ \mathbf{I}\end{bmatrix} \tag{28}$$

in which I_t = sum of the mass moments of inertia of all the masses including the base mass. The components of system matrices for a single story isolated structure have been described in the Appendix. The total frictional force acting at CSI can be assumed to resist the resultant sliding velocity at the CM of base mass. The direction of components of the frictional force acting at the CM is governed by three signum functions, two for the translational components and one for the rotational component. The vector containing the frictional forces is given by

$$\mathbf{\mu_f} = \begin{Bmatrix} f_{fx}\,\mathrm{sgn}(\dot{x}_b) \\ f_{fy}\,\mathrm{sgn}(\dot{y}_b) \\ f_{f\theta}\,\mathrm{sgn}(\dot{\theta}_b) \end{Bmatrix} \tag{29}$$

The magnitudes of the frictional force components can be determined by evaluating the direction of sliding velocity of the CM of base mass using the expressions given below

$$f_{fx} = m_t \mu g \cos \upsilon$$
$$f_{fy} = m_t \mu g \sin \upsilon \tag{30}$$

The component $f_{f\theta}$ = moment produced by the above components. The signum functions have the value of either $+1$ or -1 and are determined from

$$\mathrm{sgn}(\dot{x}_b) = -\frac{f_{Ix} + f_{Rx}}{|f_{Ix} + f_{Rx}|}$$
$$\mathrm{sgn}(\dot{y}_b) = -\frac{f_{Iy} + f_{Ry}}{|f_{Iy} + f_{Ry}|} \tag{31}$$
$$\mathrm{sgn}(\dot{\theta}_b) = -\frac{f_{I\theta} + f_{R\theta}}{|f_{I\theta} + f_{R\theta}|}$$

In order to take advantage of the normal modes of the superstructure and thereby reduce computational efforts, mode-synthesis approach has been utilized in solving the equations of motion (Singh and Suarez 1992). The modal properties of the superstructure are assumed to remain unaltered during the sliding phase and have been used for modal decomposition. Due to the nonclassically damped behavior of the structure in this phase of motion, complex modal analysis has been used to uncouple the equations and the final solution has been obtained using step-by-step integration procedures (Pranesh 2000; Pranesh and Sinha 2000a).

Direction of Sliding

The direction of sliding at any instant is partly defined by the angle υ of CM of base with respect to the coordinate system and is given by Eq. (22). In addition to the angle υ, values of the signum functions for the two principal directions completely define the direction of sliding. The values of signum functions at the beginning of a sliding phase can be determined using Eq. (31).

End of Sliding Phase

The end of a sliding phase is governed by the condition that translational and rotational sliding velocities of the base are simultaneously equal to zero. Unless all components of velocity are zero, the structure remains in sliding phase. So, the condition for the end of sliding phase is

$$\dot{\mathbf{x}}_\mathbf{b} = \mathbf{0} \tag{32}$$

Once all the components of sliding velocity are zero, the structure may enter a nonsliding phase, reverse its direction of sliding, or have a momentary stop and continue in the same direction. To decide the correct state of motion, the solution process is continued in the next time increment using the equations of nonsliding phase wherein the sliding acceleration is made equal to zero and the validity of inequalities (21) and (24) are checked to determine the possibility of sliding. If these inequalities are satisfied at the same instant of time when all components of sliding velocity are zero, it implies that there is a momentary stop at that instant of time. Eqs. (22) and (31) are used to decide the direction of sliding in subsequent time increments.

Torsional System Parameters

In the present study a one-story structure with square plan has been considered. The structure consists of a rigid roof slab supported on four columns, and the columns are connected to a rigid base slab. The base slab is supported on four identical sliding-type isolators located below each column. The schematic plan and elevation view of the structural model is shown in Fig. 3. Structural deformations are represented using 3 DOF (two translational and one rotational) at the base slab and roof slab levels. If the column masses are included in the slab mass and columns are modeled as massless, the geometric center of the slab corresponds to the CM of the structure at that level. The center of stiffness at the roof slab level depends on the relative stiffness of each column. The center of stiffness of the base slab is a function of isolator displacement as has been discussed earlier.

The main parameters affecting the torsional coupling are the values of uncoupled lateral and torsional frequencies of the superstructure and the eccentricity between the mass center and the stiffness center. The uncoupled frequencies of the superstructure in the three co-ordinate directions can be defined as

$$\omega_{s_x} = \sqrt{\frac{K_x}{M_s}}, \quad \omega_{s_y} = \sqrt{\frac{K_y}{M_s}}$$
$$\omega_{s_\theta} = \sqrt{\frac{K_\theta}{M_s r_s^2}} \tag{33}$$

where K_x, K_y, and K_θ = stiffness coefficient of the fixed-base structure in X, Y, and θ directions, respectively; M_s = mass of the superstructure; and r_s = radius of gyration of the roof slab. The uncoupled frequencies of the isolation system are defined in a similar way and are given below

$$\omega_{b_x} = \sqrt{\frac{K_b}{M_t}}, \quad \omega_{b_y} = \sqrt{\frac{K_b}{M_t}}$$

and

$$\omega_{b_\theta} = \sqrt{\frac{K_{b_\theta}}{M_t r_b^2}} \tag{34}$$

where r_b = radius of gyration of the base mass and M_t = total mass of the structure including the base mass. The extent of coupling of lateral and torsional motions depends on relative values of these frequencies. So, it is appropriate to define two uncoupled frequency ratios for the superstructure and the isolation system as below.

Superstructure:

$$\Omega_{s_x} = \frac{\omega_{s_\theta}}{\omega_{s_x}}$$
$$\Omega_{s_y} = \frac{\omega_{s_\theta}}{\omega_{s_y}} \tag{35}$$

Isolation system:

$$\Omega_{b_x} = \frac{\omega_{b_\theta}}{\omega_{b_x}}$$
$$\Omega_{b_y} = \frac{\omega_{b_\theta}}{\omega_{b_y}} \tag{36}$$

It should be noted that, in the case of VFPI, the frequency ratios of isolation system change with sliding displacement. From Eq.

Table 1. Damped Frequencies (Hz) in Different Modes of Vibration for Example Systems with Different Eccentricity Ratios

	Eccentricity ratio = 0.0						Eccentricity ratio = 0.15					
Ω_s	1	2	3	4	5	6	1	2	3	4	5	6
0.8	2.47	3.09	3.09	14.62	18.17	18.34	2.44	3.08	3.11	14.24	18.17	18.84
1.0	3.05	3.09	3.09	18.02	18.17	18.34	2.95	3.08	3.17	16.87	18.17	19.59
1.5	3.08	3.09	4.67	18.17	18.34	27.67	3.08	3.08	4.66	18.17	18.19	27.89

(36) it is observed that both the torsional and lateral frequencies depend on the instantaneous stiffness of the individual isolators and hence change in the stiffness with sliding does not significantly change the frequency ratio. Therefore the base frequency ratios are largely governed by the position of isolator with respect to center of mass rather than the change in stiffness due to sliding.

The other important parameters affecting the torsional response are the eccentricities of the superstructure and the isolation system. These eccentricities can be normalized with respect to radius of gyration of the roof slab to obtain the eccentricity ratios. These ratios give the extent of asymmetry with reference to the dimensions of the slab and are proper indicators of the asymmetry. The eccentricity ratios for the structure and isolation system are defined as

$$e_{s_r} = \frac{\sqrt{e_x^2 + e_y^2}}{r_s}$$
$$e_{b_r} = \frac{\sqrt{e_{bx}^2 + e_{by}^2}}{r_b} \tag{37}$$

It has to be noted that the eccentricity ratio of the isolation system changes with displacement of base mass. The variation of the eccentricity of isolation system depends primarily on the instantaneous frequencies of the different isolators and their position with respect to the CM of base mass. Depending upon the displacement at the isolators this variation can be significant. Since the present formulation considers this variation in the formulation, the presented results automatically incorporate its effect. However due to the continuous variation of isolation eccentricity during the time history of response, it is not possible to present the effect of this variation explicitly. Further it has also been observed that isolation eccentricities in sliding isolation systems do not significantly affect the structural behavior (Nagarajaiah et al. 1993).

Example Systems

In this section the effect of torsional coupling due to asymmetry of example structures has been investigated. The single story model shown in Fig. 3 has eccentricity in *y* direction and the excitation is applied in *x* direction. The top and base mass have been assumed to be equal so that mass ratio (α) is equal to 0.5. The desired degree of asymmetry is achieved by varying the stiffness offset. The study has been carried out for three uncoupled frequency ratios of the superstructure: 0.8, 1.0 and 1.5. These frequency ratios represent typically a torsionally flexible system, a system with tuned frequencies, and a torsionally stiff system, respectively. These frequency ratios encompass the variety of structures prone to torsional motions. The stiffness of the resisting elements are kept the same so that the lateral frequencies are similar while the torsional frequency is adjusted by varying the position of isolators relative to the center of mass in order to get the desired frequency ratios. The superstructure eccentricity ratio from 0.0 to 0.15 has been considered in this study. This range of eccentricity covers the asymmetry that is ordinarily found in structures. This variation in superstructure eccentricity ratio has been obtained by shifting the columns (thereby shifting the isolators) on one of the sides about the center of mass. As a result the eccentricity at the isolation level also changes. The range of isolation eccentricity ratio corresponding to the superstructure eccentricity ratio of 0.0:0.15 is 0.0–0.064.

The torsional response of the structure isolated by VFPI is determined for single story structures subjected to El Centro 1940 (NS) ground motions. In order to simulate the effect of moderate and severe earthquakes, the recorded earthquake ground motions have been multiplied with scale factors (called intensity factors in this paper) of 1.0 and 2.0. The response of the isolated structure for both levels of ground excitation has been compared with that of the fixed base structure and also with the corresponding structure isolated by FPS and PF systems. In all examples presented herein, VFPI has been chosen with frequency variation factor equal to 5.0/m. From previous studies it has been found that VFPI is more effective for range of coefficient of friction of 0.02:0.1 while FPS is found to be effective only for relatively higher coefficient of friction (Pranesh and Sinha 2002). Therefore two values of coefficients of friction have been chosen for this study, corresponding to 0.02 and 0.10. The superstructure damping ratio is assumed to be 5% of critical damping in all modes.

The damped modal frequencies of the isolated structure are given in Table 1 for the two extreme values of eccentricities 0.0 and 0.15, and for three values of frequency ratios 0.8, 1.0, and 1.5. The second frequency and the fifth frequency corresponding to the base DOF and structural DOF in *y* direction, respectively, remain unaltered since the structure is symmetrical about the *y* direction. The first and the third frequencies are the coupled lateral and torsional frequencies of the base DOFs. For frequency ratios of 0.8 and 1.0 the fourth and the sixth superstructure frequencies are coupled, whereas fifth and sixth frequencies are coupled when frequency ratio is 1.5. From these values it is observed that the coupled frequencies move away from each other with increase in eccentricity ratio. It is also important to observe that the torsional to lateral frequency ratio of the isolation system is directly dependent on the ratio of the superstructure natural frequencies.

Behavior of Variable Frequency Pendulum Isolator under Earthquake Loading

The typical time history response of a torsionally coupled single story structure isolated by VFPI is shown in Fig. 5 for eccentricity ratio of 0.05 and a frequency ratio of unity. Time history responses for the same structure isolated by FPS and PF systems are also shown in this figure for comparison purpose. Since the VFPI is effective for both moderate and high levels of excitation, the response has been presented for El Centro ground motion scaled by an intensity factor of 2.0. As per the available records the duration of strong motion shaking during the earthquake was 30 s, and the same has been taken as the duration of ground motion.

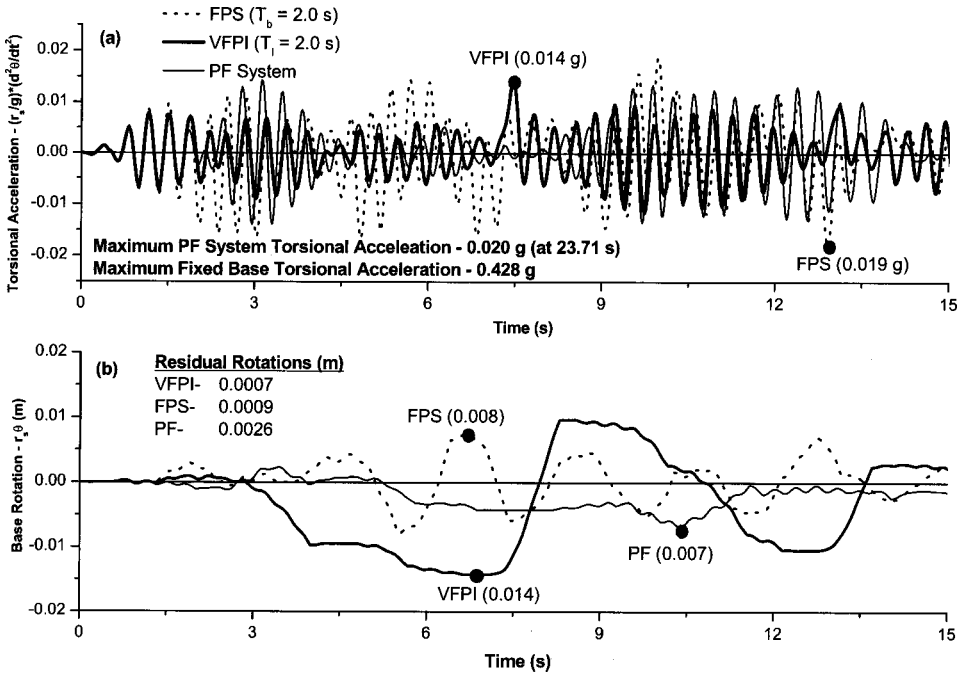

Fig. 5. Time history torsional response of example structure subjected to El Centro ground motion scaled to twice intensity

The torsional acceleration has been normalized with radius of gyration and the acceleration due to gravity so as to get the acceleration in units of *g*. The torsional rotations are normalized with radius of gyration so as to represent the results in units of linear displacement. This also quantifies the torsional motions for comparison with lateral motions. From Fig. 5(a), it can be observed that the torsional accelerations for structure isolated by VFPI are significantly lower than those for structure isolated by FPS. This is primarily due to the restoring-force softening in VFPI being significant for high levels of excitation. Fig. 5(b) shows the rotational displacements of the center of base mass. From this result, it can be observed that the maximum displacement of structure with VFPI is higher than with other isolation systems. This is due to the force softening mechanism in VFPI permitting larger displacements. However it is found that the residual rotations of the base mass are very low for structure with VFPI when compared to the PF system, since the lower restoring force in VFPI is effective in bringing the structure back to its original position. The residual rotations for structure with the PF system are substantially greater due to its lack of restoring force mechanism.

The biaxial motion of the center of base mass and motion of all four isolators for El Centro 1940 (NS) ground motion are shown in Figs. 6 and 7, respectively. For this analysis the critical case of excitation, when the ground motion is at an angle of 45° with the principal axes of the structure, has been used (along the line joining Isolator 1 and Isolator 3 in Fig. 3). The eccentricity ratio is 0.05 in *Y* direction, signifying a structure with moderate torsional coupling. From Fig. 7 it is observed that isolators along the line of excitation have significant motions perpendicular to the excitation direction, which indicates the influence of rotational motions. The motion of isolators perpendicular to the direction of excitation (Isolators 2 and 4) is predominately in the excitation direction. This is due to the square geometry of the base mass chosen for the example system, wherein the perpendicular direction to the axis joining Isolators 2 and 4 is collinear with the excitation direction. Since rotational motion of these isolators takes place perpendicular to the axis joining Isolators 2 and 4, this motion adds to the sliding along the excitation direction and cannot be shown separately. It is therefore clearly observed that while an individual isolator may have significant torsional motions, the motion of center of base mass is predominantly in the direction of excitation. This characteristic of torsional behavior of structure isolated using VFPI can be further elaborated by examining the time history of isolator motions parallel and perpendicular to the direction of ground excitation. The isolator displacement time his-

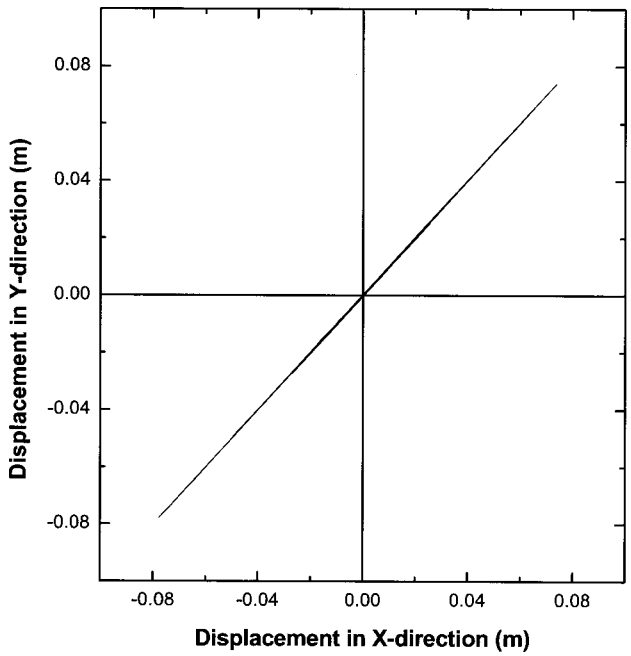

Fig. 6. Displacement orbits of center of base mass of the example structure subjected to El Centro ground motion acting at 45° to principal direction

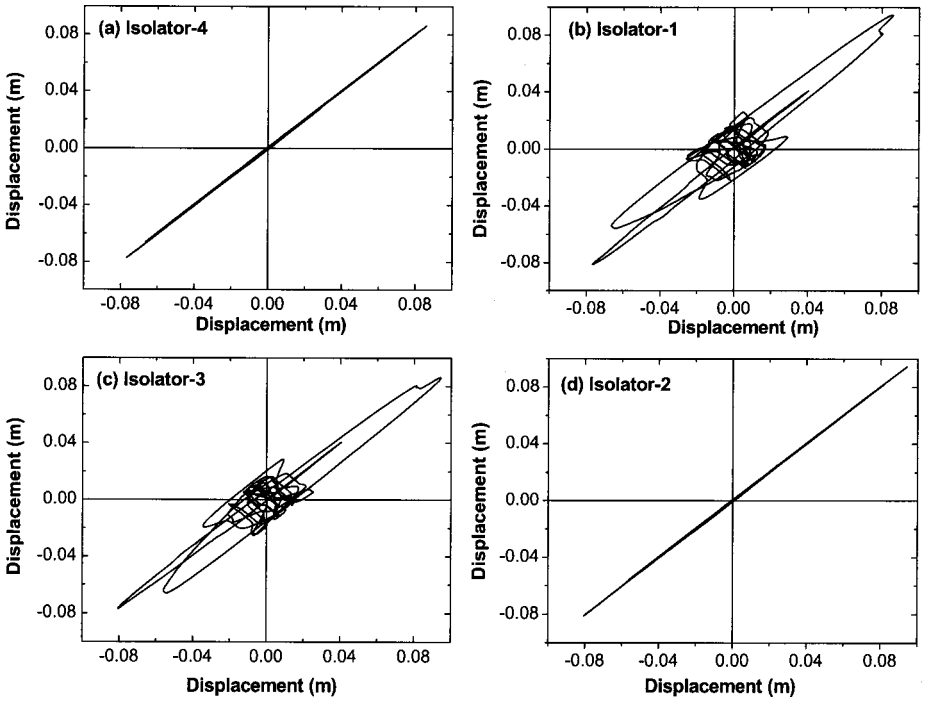

Fig. 7. Displacement orbits of individual variable frequency pendulum isolator isolators in example structure subjected to El Centro ground motion acting at 45° to principal direction

tories have been shown in Fig. 8. It is again observed that the displacement perpendicular to excitation direction is significant only in Isolators 1 and 3. It is also further observed that these displacements are of almost equal and opposite magnitude so that their net effect on the displacement of the CM is insignificant. This results in base mass motion almost exclusively in the direction of excitation, and the effect of torsional motion is negligible even for torsionally coupled structures (Fig. 7).

The performance of isolated structures to near field ground motions is of particular interest due to their pulse-like motions. To illustrate the performance of VFPI under near field ground motions, the time history of torsional acceleration and base rotations

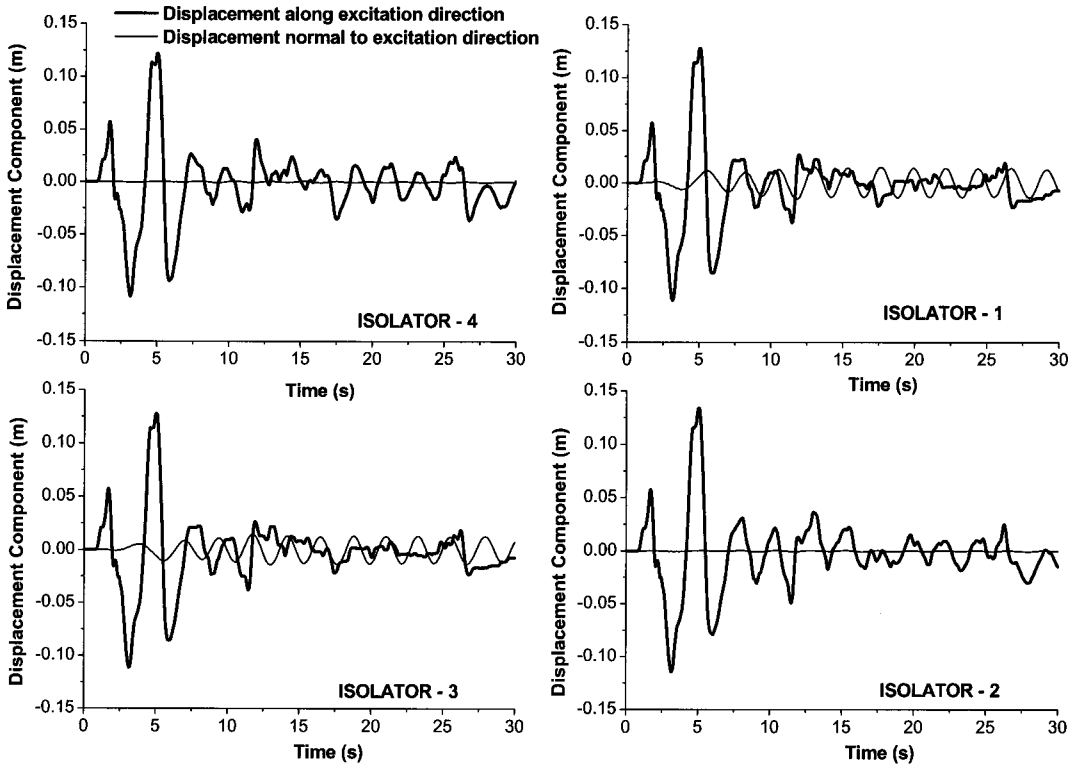

Fig. 8. Time histories of displacements of individual isolators along and normal to direction of El Centro ground motion acting at 45° to principal direction

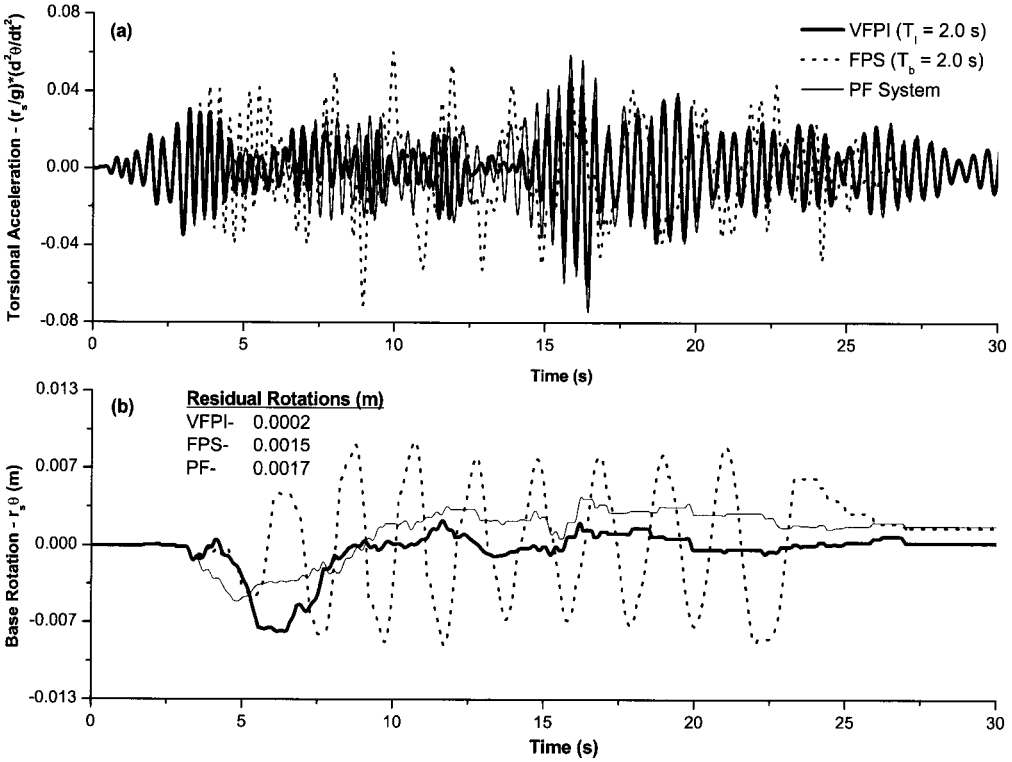

Fig. 9. Time history torsional response of example structure subjected to Northridge (Sylmar) ground motion

of the example structure when subjected to the Sylmar component of Northridge Earthquake (1994) are presented in Fig. 9. It can be observed that there is a substantial decrease in the acceleration of structure isolated with VFPI without the corresponding increase in sliding displacement. Most of the peaks found in acceleration response of the FPS-isolated structure are filtered out in the case of VFPI-isolated structure. It is also interesting to note that the oscillatory rotational sliding characteristic of FPS is not observed for VFPI and PF systems. Further the residual displacements in VFPI are much less than those found in FPS and PF systems. The typical response of structure isolated using VFPI when subjected to near-field ground motions also clearly shows its superiority of VFPI in comparison with the other sliding isolation systems.

It is necessary to emphasize here that in the case of VFPI the initial time period and FVF are the two important isolator parameters which control the acceleration and displacement responses. Initial time period controls the initial stiffness (required for small intensity earthquakes) while FVF decides the rate of change of frequency with respect to displacement and hence controls the acceleration and displacement response. Although decrease in acceleration results in a corresponding increase in sliding displacement in most isolators, this is not entirely true in the case of VFPI. This is because VFPI has a bounded restoring force and hence there is a total decrease in the energy input, which will govern the increase in displacement. This is not possible in most other types of isolators as the energy input increases with both increase in acceleration and displacements. Table 2 shows the maximum torsional acceleration and displacement responses of the example structure isolated by two VFPI isolators subjected to different earthquake records. The corresponding linear response is given in Table 3. The two isolators have same initial time period of 2 s but with different FVF values (and corresponding rate of variation of time period). The VFPI-1 has FVF of 7/m and VFPI-2 has FVF equal to 5/m. The maximum response of the structure isolated by FPS with time period 2 s has also been shown for reference purposes. From these results it is seen that the response characteristics of isolated structure can be controlled due to the ability to choose different isolator parameters of VFPI as per requirements. It is also observed that VFPI is quite effective under a variety of earthquake excitations.

Effect of Asymmetry on Torsional Moment

The effect of torsion on design forces is predominately due to additional shear force introduced in the columns or the lateral force resisting elements. The shear force due to torsion depends on the distance of the individual column from the center of mass and may increase or reduce the shear due to other forces. The effect of lack of symmetry on torsional response has been studied by considering the variation of maximum torsional moment with eccentricity ratio, as shown in Figs. 10(a–c). Here the example systems are subjected to El Centro ground motion scaled to intensity factor of 2.0. The response quantities are shown for structures isolated with VFPI, FPS, and PF systems, all with coefficient of sliding friction of 0.02. In the results presented, frequency ratios of 0.8, 1.0, and 1.5 have been considered so as to encompass the practical range of torsional stiffness. The maximum values of torsional moments normalized with respect to corresponding values for fixed base structure are also shown in Figs. 10(d–f).

It is found from Figs. 10(a–c) that, as expected in all cases, the torsional moment steadily increases with increase in the eccentricity ratio. From these curves it is interesting to note that VFPI behaves better than both FPS and PF systems for frequency ratio up to unity. The FPS system is found to produce maximum torsional response at all frequency ratios. This is due to the higher restoring force produced in FPS isolators that induce larger torsional moments in the structure. From Figs. 10(d–f), it is further

Table 2. Maximum Torsional Response of Example Structure Subjected to Different Earthquake Excitations

Structure no.	Earthquake record	Torsional acceleration$\times r/g$ (10^{-3} g)			Sliding rotation$\times r$ (10^{-3} m)			Residual rotation$\times r$ (10^{-3} m)		
		VFPI-1[a]	VFPI-2[a]	FPS[b]	VFPI-1[a]	VFPI-2[a]	FPS[b]	VFPI-1[a]	VFPI-2[a]	FPS[b]
1	Imperial Valley, 1940 (270°)	13.32	13.48	16.24	3.44	3.72	2.70	0.418	0.411	0.388
2	Imperial Valley, 1940 (180°)	16.13	17.80	20.06	4.40	6.47	3.83	0.380	0.360	0.402
3	Taft, 1952 (339°)	14.89	17.27	13.36	2.20	2.47	1.58	0.717	0.727	0.720
4	Loma Prieta, 1989 (270°)	11.91	11.36	15.84	2.67	2.13	3.00	0.096	0.117	0.200
5	Northridge (Sylmar), 1994	17.53	20.31	23.65	5.74	7.28	8.78	0.193	0.234	1.52
6	San Fernando (8244 Orion Blvd.), 1971 (180°)	15.20	13.75	16.20	5.32	5.68	3.50	0.806	0.360	0.790
7	San Fernando (Pacoima Dam), 1971 (286°)	23.74	41.42	34.58	17.2	80.9	15.0	0.923	1.03	2.60
8	Parkfield (Cholame Shandon), 1966 (40°)	16.01	15.78	15.19	1.64	1.63	1.79	1.08	1.05	0.972
9	Mexico City, 1985	20.40	14.71	122.4	14.2	6.71	31.6	0.047	0.150	0.027

[a]Variable frequency pendulum isolator.

[b]Friction pendulum system.

observed that there is a substantial reduction in the torque for all isolated structures in comparison with conventional fixed base structure. It is also seen that the maximum effectiveness of isolation system in reducing torsional response is when the frequency ratio is unity. However, it is important to note that the structure with VFPI behaves significantly better than that with FPS for all frequency ratios. It is also found that FPS transmits higher torsional moment than VFPI and the PF system for torsionally stiff structural systems [Figs. 10(c and e)]. This example system clearly illustrates the effectiveness of VFPI in comparison with the FPS and PF systems in reducing torsional response of isolated structures.

Effect of Frequency Ratio on Torque Amplification

The effect of torsional coupling can be qualitatively evaluated by investigating the extent of dynamic amplification of the torque in comparison with the static torque. The primary variable can be taken as the ratio of dynamic torque to the static torque and has been termed as the torque amplification factor (TAF) (Nagarajaiah et al. 1993). The static torque is defined as the product of the resultant shear obtained from the dynamic analysis multiplied by the static eccentricity. So, the ratio of the dynamic torque to this static torque gives the extent of torque amplification during dynamic response and is a direct measure of the extent of torsional coupling.

To study the amplification of torque, spectra of the amplification factor are plotted against the frequency ratio for El Centro 1940 (NS) ground motion scaled with intensity factors 1.0 and 2.0 and for coefficients of sliding friction 0.02 and 0.10 (Fig. 11). The eccentricity ratio has been taken as 0.05 during this evaluation. The torque amplification factors are also plotted for other sliding isolation systems and fixed base systems for comparison. As the TAF depends on both the base shear and the dynamic torque, a lower or higher value of the same does not indicate the efficiency of an isolation system in resisting the torsional forces. This factor is an indicator of the effectiveness of the isolation system in resisting the torsional motions in comparison with the lateral motions. For a given eccentricity, lateral motions are represented by base shear whereas torsional motions by dynamic torque. Therefore values of TAF primarily indicates the extent of coupling of

Table 3. Maximum Linear Response of Example Structure Subjected to Different Earthquake Excitations

Structure no.	Earthquake record	Acceleration (10^{-3} g)			Sliding displacement (10^{-3} m)			Residual displacement (10^{-3} m)		
		VFPI-1[a]	VFPI-2[a]	FPS[b]	VFPI-1[a]	VFPI-2[a]	FPS[b]	VFPI-1[a]	VFPI-2[a]	FPS[b]
1	Imperial Valley, 1940 (270°)	92.07	89.93	149.0	129.4	148.2	119.5	2.67	2.60	2.50
2	Imperial Valley, 1940 (180°)	93.17	88.32	138.8	252.8	245.1	111.4	1.02	0.90	1.00
3	Taft, 1952 (339°)	87.80	87.70	87.90	44.71	42.60	39.12	0.82	0.80	0.60
4	Loma Prieta, 1989 (270°)	99.00	101.2	151.9	91.26	103.1	130.2	3.23	3.10	2.90
5	Northridge (Sylmar), 1994	77.06	92.37	625.1	269.0	306.2	508.0	0.192	0.20	0.00
6	San Fernando (8244 Orion Blvd.), 1971 (180°)	85.4	85.5	176.0	195.8	214.5	155.3	2.34	2.50	2.20
7	San Fernando (Pacoima Dam), 1971 (286°)	95.46	83.88	620.7	579.5	554.3	483.5	1.41	5.40	0.00
8	Parkfield (Cholame Shandon), 1966 (40°)	70.60	69.61	66.14	16.04	15.95	15.62	4.30	4.20	3.90
9	Mexico City, 1985	81.57	97.75	1910.0	328.7	331.3	841.6	1.58	1.60	1.50

[a]Variable frequency pendulum isolator.

[b]Friction pendulum system.

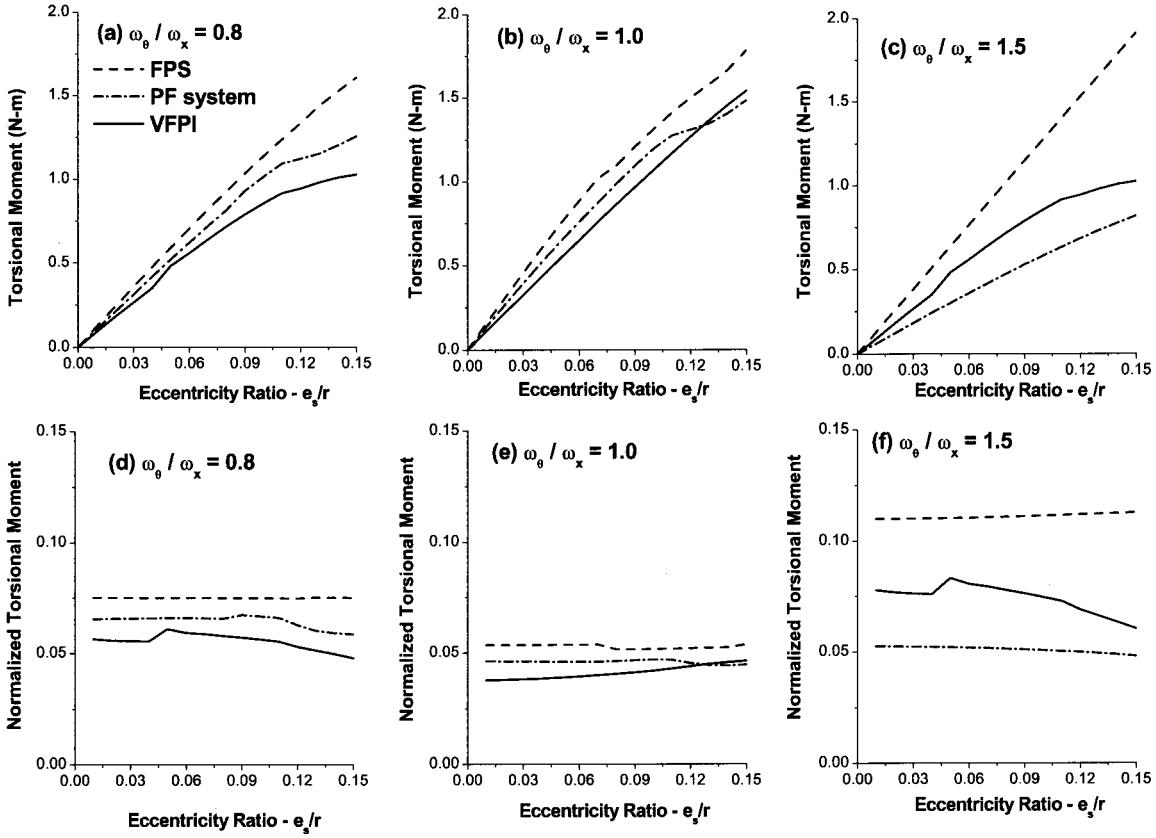

Fig. 10. Effect of eccentricity on torsional response of example structure subjected to El Centro ground motion scaled to twice intensity: (a)–(c) torsional moment per unit structure mass; (d)–(f) normalized torsional moment

translation and rotation response for a given isolation system.

From Fig. 11, it is seen that the coupling effect is most significant when the frequency ratio is near unity in all cases, and it reduces for frequency ratios other than unity. It is further observed that in the case of lower coefficient of friction and higher intensity of excitation [Fig. 11(c)], the maximum torque amplification occurs at a higher frequency ratio for structure isolated by VFPI. This is because of significant reduction in torsional frequency of the structure isolated using VFPI for high isolator displacements. Since the torsional effects are quantified by TAF, which depend both on the static and the dynamic torque in the same type of isolator, the comparison of TAF for different types

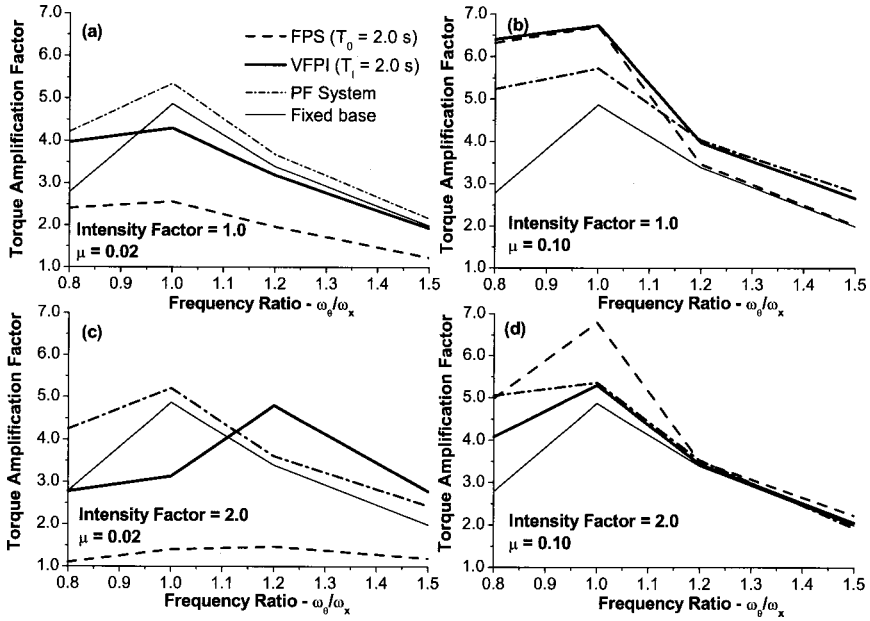

Fig. 11. Effect of frequency ration on torque amplification factor for example structure subject to El Centro ground motion

Table 4. Static Torque Per Unit Structural Mass for Example Systems with Frequency Ratio of Unity and Different Coefficient of Sliding Friction

	Intensity factor = 1.0		Intensity factor = 2.0	
Isolator	$\mu = 0.02$	$\mu = 0.10$	$\mu = 0.02$	$\mu = 0.10$
VFPI[a]	0.0124	0.0420	0.0146	0.0576
FPS[b]	0.0208	0.0419	0.0426	0.0488
PF system[c]	0.0106	0.0437	0.0116	0.0527
Fixed-base	0.1320		0.2640	

[a]Variable frequency pendulum isolator.

[b]Friction pendulum system.

[c]Pure friction.

of isolators will not illustrate the true behavior of the different isolator types. It is therefore necessary to observe the static torque values independently for different isolators. The static torque per unit mass for the example system with different coefficient of friction is given in Table 4. From this table, it can be observed that for low coefficient of friction ($\mu = 0.02$) the static torques in the case of VFPI and PF systems are significantly lower than those in the case of FPS. Therefore higher TAF in the case of VFPI and PF systems in comparison with that of FPS indicate that the torsional coupling is significant in these isolators for both levels of excitation [Figs. 11(a and c)]. In the case of spectra with higher coefficient of friction [Figs. 11(b and d)] the torsional coupling is more significant for FPS than that for VFPI, especially for high levels of excitation. Further it can be observed from Table 4 that for $\mu = 0.10$, there is insignificant variation in the magnitude of static torque for different isolation systems. From this it can be concluded that the effect of torsional coupling is more significant for higher coefficient of friction for FPS and VFPI. The magnitude of torsional coupling is particularly significant for FPS in the case of high intensity of excitation.

To summarize, it has been observed that the torsionally coupled structures isolated using FPS have inherent disadvantages when subjected to high intensity base excitations. For low coefficient of sliding friction the maximum lateral motions of structures isolated with FPS are significant, resulting from high restoring force, although the effect of torsional coupling is low. Use of higher coefficient of sliding friction helps in control of lateral motions but leads to significantly higher torsional coupling due to the constant isolator time period of FPS. These disadvantages of FPS can be minimized by the use of VFPI while retaining the main advantages of FPS.

Summary and Conclusions

The mathematical formulation for a generalized 3D structure isolated by a sliding isolation system with nonlinear restoring force has been presented in this paper. This formulation focuses on the response of structure isolated using VFPI. The key parameters that influence the 3D behavior of asymmetric structures isolated by sliding type isolators have been identified. It has been found that the most important parameters affecting torsional response are: (1) uncoupled torsional to lateral frequency ratio, (2) superstructure eccentricity between CM and CR, and (3) coefficient of sliding friction. Examples of asymmetric single story structures isolated using VFPI, FPS, and PF system have been analyzed to study their torsional behavior.

Based on these investigations, the following main conclusions can be drawn:

1. the effect of torsional coupling on the response of structures can be very significant and needs to be considered in the analysis of isolated asymmetric structures;
2. substantial reduction in the torsional response can be achieved by isolating the structures by sliding-type isolators;
3. the effect of torsional coupling is greater for higher coefficient of sliding friction of the isolator;
4. the torsional behavior of structures isolated by VFPI is significantly better than other sliding-type isolators, especially for high intensity of excitation; and
5. higher eccentricity between CM and CR leads to higher torsional motions. However, the motion of the center of mass of the structure remains substantially unidirectional in the direction of excitation when the structure is isolated using VFPI.

Appendix. System Matrices for Single Degree of Freedom Structure in Sliding Phase

The equations of motion of a single story structure in sliding phase are given by Eq. (19), in which the global matrices contain structural submatrices for the fixed base structure and the submatrices corresponding to isolator DOF. The matrices in equations of motion can be written in terms of the 6 DOF (three corresponding to base mass and three to structure mass) as

$$\mathbf{M}=\begin{bmatrix} m_s & 0 & 0 & m_s & 0 & 0 \\ 0 & m_s & 0 & 0 & m_s & 0 \\ 0 & 0 & I_s & 0 & 0 & I_s \\ m_s & 0 & 0 & m_t & 0 & 0 \\ 0 & m_s & 0 & 0 & m_t & 0 \\ 0 & 0 & I_s & 0 & 0 & I_t \end{bmatrix}$$

$$\mathbf{C}=\begin{bmatrix} C_x & 0 & 0 & 0 & 0 & 0 \\ 0 & C_y & 0 & 0 & 0 & 0 \\ 0 & 0 & C_\theta & 0 & 0 & 0 \\ 0 & 0 & 0 & C_{b_{xx}} & 0 & -C_{b_{x\theta}} \\ 0 & 0 & 0 & 0 & C_{b_{yy}} & C_{b_{y\theta}} \\ 0 & 0 & 0 & -C_{b_{x\theta}} & C_{b_{y\theta}} & C_{b_{\theta\theta}} \end{bmatrix}$$

$$\mathbf{K}=\begin{bmatrix} K_x & 0 & 0 & 0 & 0 & 0 \\ 0 & K_y & 0 & 0 & 0 & 0 \\ 0 & 0 & K_\theta & 0 & 0 & 0 \\ 0 & 0 & 0 & K_{b_{xx}} & 0 & -K_{b_{x\theta}} \\ 0 & 0 & 0 & 0 & K_{b_{yy}} & K_{b_{y\theta}} \\ 0 & 0 & 0 & -K_{b_{x\theta}} & K_{b_{y\theta}} & K_{b_{\theta\theta}} \end{bmatrix}$$

$$\mathbf{x}=\begin{Bmatrix} x_s \\ y_s \\ \theta_s \\ x_b \\ y_b \\ \theta_b \end{Bmatrix}, \quad \mathbf{r}=\begin{bmatrix} 0 & 0 & 0 \\ 0 & 0 & 0 \\ 0 & 0 & 0 \\ 1 & 0 & 0 \\ 0 & 1 & 0 \\ 0 & 0 & 1 \end{bmatrix}$$

$$\ddot{\mathbf{x}}_\mathbf{g} = \begin{Bmatrix} \ddot{x}_g \\ \ddot{y}_g \\ \ddot{\theta}_g \end{Bmatrix} \tag{38}$$

where m_s = mass of fixed base structure; m_t = total mass of the structure including the base mass; I_t = total mass moment of inertia of both the masses; and C_x, C_y, and C_θ = damping coefficients of the structure in the three principal directions. The damping coefficients with suffix b are used to denote the total equivalent damping at isolator level in the respective direction. The presence of eccentricity causes coupling between translational and rotational degrees of freedom at the base level. This formulation for eccentrically coupled structure is similar to Goel and Chopra (1990) and has been extended herein to include sliding isolators.

References

Buckle, I. G., and Mayes, R. L. (1990). ''Seismic isolation: History, application and performance—a world view.'' *Earthquake Spectra*, 6(2), 161–201.

Chopra, A. K. (2000). *Dynamics of structures: Theory and applications to earthquake engineering*, 2nd Ed., Prentice–Hall, Upper Saddle River, N.J.

Goel, R. K., and Chopra, A. K. (1990). ''Inelastic seismic response of one-story asymmetric-plan systems: Effect of stiffness and strength distribution.'' *Earthquake Eng. Struct. Dyn.*, 19(7), 949–970.

Jangid, R. S., and Datta, T. K. (1994). ''Nonlinear response of torsionally coupled base isolated structure.'' *J. Struct. Eng.*, 120(1), 1–22.

Kelly, J. M. (1986). ''Aseismic base isolation: Review and bibliography.'' *Soil Dyn. Earthquake Eng.*, 5(4), 202–216.

Kelly, J. M. (1993a). *Earthquake resistant design with rubber*, Springer, London.

Kelly, J. M. (1993b). ''State-of-the-art and state-of-the-practice in base isolation.'' *Proc., ATC-17-1 Seminar on Seismic Isolation, Passive Energy Dissipation, and Active Control; Volume 1: Seismic Isolation Systems*, Applied Technology Council, Redwood City, Calif. 9–28.

Lee, D. M. (1980). ''Base isolation for torsional reduction in asymmetric structures under earthquake loading.'' *Earthquake Eng. Struct. Dyn.*, 8(4), 349–359.

Mostaghel, N., and Tanbakuchi, J. (1983). ''Response of sliding structures to earthquake support motion.'' *Earthquake Eng. Struct. Dyn.*, 11(6), 729–748.

Naeim, F., and Kelly, J. M. (1999). *Design of seismic isolated structures: From theory to practice*, Wiley, New York.

Nagarajaiah, S., Reinhorn, A. M., and Constantinou, M. C. (1993). ''Torsional coupling in sliding base-isolated structures.'' *J. Struct. Eng.*, 119(1), 130–149.

Pan, T. C., and Kelly, J. M. (1983). ''Seismic response of torsionally coupled base-isolated structures.'' *Earthquake Eng. Struct. Dyn.*, 11(6), 749–770.

Pranesh, M. (2000). ''VFPI: An innovative device for aseismic design.'' Ph.D. thesis, Indian Institute of Technology, Bombay, India.

Pranesh, M., and Sinha, R. (2000b). ''Aseismic design of tall structures using variable frequency pendulum isolator.'' *Proc., 12th World Conf. on Earthquake Engineering*, Auckland, New Zealand, Paper No. 284.

Pranesh, M., and Sinha, R. (2000a). ''VFPI: An isolation device for aseismic design.'' *Earthquake Eng. Struct. Dyn.*, 29(5), 603–627.

Pranesh, M., and Sinha, R. (2002). ''Earthquake resistant design of structures using the variable frequency pendulum isolator.'' *J. Struct. Eng.*, 128(7), 870–880.

Singh, M. P., and Suarez, L. E. (1992). ''Dynamic condensation with synthesis of substructure eigenproperties.'' *J. Sound Vib.*, 159(1), 139–155.

Sinha, R., and Pranesh, M. (1998). ''FPS isolator for structural vibration control.'' *Proc., Int. Conf. on Theoretical, Applied, Computational, and Experimental Mechanics* (CD), IIT, Kharagpur, India.

Sinha, R., and Pranesh, M. (2001). ''Earthquake resistant design of torsionally coupled structures using VFPI.'' *Structures 2001 Conf.: 2001 Structures Congress and Exposition Structural Engineering Odyssey*, Washington D.C.

Zayas, V. A., Low, S. S., and Mahin, S. A. (1987). ''The FPS earthquake resisting system: Experimental report.'' *Rep. No. UCB/EERC-87/01*, Earthquake Engineering Research Center, Univ. of California, Berkeley, Calif.

Zayas, V. A., Low, S. S., and Mahin, S. A. (1990). ''A simple pendulum technique for achieving seismic isolation.'' *Earthquake Spectra*, 6(2), 317–333.